Robotic Assistants for Aircraft Inspectors

Mel Siegel, Priyan Gunatilake, and Gregg Podnar
Intelligent Sensor, Measurement, and Control Laboratory
The Robotics Institute -- School of Computer Science -- Carnegie Mellon University
Pittsburgh, Pennsylvania 15213-3891

ABSTRACT

Aircraft flight pressurization/depressurization cycling causes the skin to inflate and deflate, stressing it around the rivets that fasten it to the airframe. The resulting strain, exacerbated by corrosion, drives the growth of initially microscopic cracks. To avoid catastrophe, aircraft are inspected periodically for cracks and corrosion. The inspection technology employed is ~90% naked-eye vision. We have developed and demonstrated robotic deployment of both remote enhanced 3D-stereoscopic video instrumentation for visual inspection and remote eddy current probes for instrumented inspection. This article describes the aircraft skin inspection application, how robotic deployment may alleviate human performance problems and workplace hazards during inspection, practical robotic deployment systems, their instrumentation packages, and our progress toward developing image enhancement and understanding techniques that could help aircraft inspectors to find cracks, corrosion, and other visually detectable damage.

KEYWORDS: automated robot visual NDI inspection enhanced remote stereoscopic multiresolution

1. INTRODUCTION

Pressurization and de-pressurization of an airplane during each takeoff and landing cycle causes its body to expand and contract like an inflating and deflating balloon. Cycling thus induces stress fatigue at the rivets that hold the aircraft surface skin to its frame, resulting in the growth of radial cracks. On April 28, 1988 Aloha Airlines flight 243, flying at 24,000 feet near Maui, abruptly lost a section of its upper fuselage skin from the floorline on the left side to the windowline on the right side, from just behind the passenger door to just in front of the wing, a distance of about 6 m [18 ft]. Although there were numerous injuries and one death (a cabin attendant was blown out during the initial decompression) the airplane landed intact except for the initial damage. The NTSB investigation[1] attributed the catastrophe to a previously unanticipated failure mode now called "multiple site damage" or MSD. In plain English, MSD means "two small cracks that joined to make one big crack"; since crack growth rate is essentially exponential in crack length, one big crack is much worse than two small cracks.

In the aftermath of "Aloha'88" Congress mandated an FAA Aging Aircraft Research Program, with a significant focus on inspection technology. By 1995 the specific aging aircraft infrastructure issues that led to Aloha'88 were declared "behind us", and the nominal emphasis shifted from "aging aircraft" to "continued airworthiness assurance". Nevertheless, in the November 3, 1997 issue of Aviation Week & Space Technology, we read that on October 27 the FAA "ordered stringent inspections and modifications to the oldest Boeing 737s flying" in response to "receiving reports from Boeing and airlines of widespread cracking in adjacent rivet holes in lap joints on the fuselage *lower* lobes of older aircraft"[2]. We emphasize *lower* in this quote because until now interest in skin cracking has focused on the upper portions of the fuselage, where there is less strengthening substructure. It is thus apparent that, name change notwithstanding, a need still exists for research on aging aircraft inspection technology.

Early in the Aging Aircraft Research Program, CMU won an FAA grant to generate and analyze scenarios for robotic deployment of instrumentation to inspect for cracks of the sort that led to the Aloha'88 incident, to design a robotic system that implemented the most promising scenario, and to prototype an initial system to demonstrate this system's feasibility. The ANDI (**A**utomated **N**on**D**estructive **I**nspector) system, discussed in detail in Section 4.1 emerged from this effort. In addition, at least four more robots for aircraft skin inspection have been built in the US: one funded by the FAA at Wichita State University (ROSTAM), one funded primarily by the Ben Franklin Technology

Center of Western Pennsylvania at CMU (CIMP), one funded by the Air Force at NASA JPL (MACS), and one privately funded by AutoCrawler LLC (AutoCrawler). [See sidebar ***other robots that crawl on airplanes*** for photos and descriptions of ROSTAM, MACS, and AutoCrawler; the second CMU robot, CIMP, is described in detail in Section 4.2.] Outside the US, the Singapore Air Force is currently supporting a substantial effort for robotic underwing inspection of F-5 aircraft, and there are persistent rumors of one or more ongoing efforts, particularly in Japan, that are not being reported in the open literature.

In the aggregate, the five US prototypes have demonstrated all of the technical capabilities needed to implement a robotically assisted inspection system: ***measurement***, ***manipulation***, ***mobility***, and ***monitoring***. [See sidebar ***the 4-Ms of robot assisted aircraft inspection*** for a diagrammatic explanation of this hierarchy.] However no system has demonstrated all "4-Ms" at once. Probably only one robot, CIMP, has actually delivered to an aircraft inspector in the field anything that could with a straight face be called useful inspection data; however CIMP, the **C**rown **I**nspection **M**obile **P**latform, succeeds in this goal (and the secondary goal of wireless operation) only by employing a design that restricts its mobility, as its name implies, to the aircraft crown, i.e., the upper fuselage, from cockpit to tail, from windowline to windowline.

2. CURRENT AND ALTERNATIVE AIRCRAFT INSPECTION METHODS

Visual inspection, augmented by instrumented inspection of known problem areas and instrumented confirmation of visually detected apparent problems, is required to ensure the structural integrity of an aircraft's skin and its supporting substructure. A "major" inspection might be carried out on a commercial aircraft every 6 years, 24,000 flying hours, or 12,000 takeoff and landing cycles; in these 6 years, there might also be 2 cycles of alternating "light" and "heavy" checks. Additional checks, primarily visual, are made during "line maintenance", which occurs each night; large aircraft that fly long routes, e.g., 747s, may also undergo a "turnaround check" each cycle. Details vary greatly from airline to airline, and within any one airline the fine structures of policies and schedules are likely to change with every upper management shuffle, but these typical figures accurately convey the spirit of how inspection and maintenance are scheduled.

Skin inspections are currently about 90% visual and 10% nondestructive inspection (NDI, meaning inspection using electronic instruments). Eddy current probes are the main NDI technology used for skin inspection. Although eddy current sensing is a near-surface sensitive technology, some depth resolution can be achieved by varying the excitation and detection frequency: the highest frequencies probe a thin layer just inside the skin surface, whereas lower frequencies and skillfully defined protocols can detect defects in second and third skin layers, and often in the ribs to which the skin is affixed.

Without exception, these inspections now require putting a human inspector on the body of the aircraft to closely examine its surface both for known structural problems and for more widespread defects, such as cracks, corrosion, damaged rivets, and lightning strikes. The practice raises safety issues for the inspector, is time consuming, and suffers at times from being ineffective due to inspector fatigue or boredom. Visual and NDI inspection practices are detailed in two sidebars, ***visual inspection: how it works***, and ***instrumented (NDI) inspection: how it works***, and illustrated by Figure 1.

Figure 1: Aircraft inspector (with flashlight and 10x magnifier) and author P.G. inspecting the crown of a Boeing 737 airplane. Note safety harnesses.

3. WHY USE A ROBOT FOR AIRCRAFT INSPECTION?

Numerous hypothesized advantages of computer controlled mobile remote deployment platforms (for short, “robots”) for aircraft inspection instruments and remote cameras for visual inspection have been expounded at length elsewhere, for example References 3, 4, and 5, and other references therein. In contrast to most of these theoretical arguments, real experience has led us to believe that robotic deployment of inspection equipment has clear operational and economic advantages over manual deployment for three really crucial reasons: ***thoroughness***, ***correctness***, and ***recordability***. Early theoretical arguments, particularly those relating to increased bodily safety of the inspectors and other advantages of “getting the man off the airplane,” now seem less plausible as the likely deployment scenario (primarily during heavy maintenance) and the personalities of the inspectors (they tell us they enjoy being on the airplanes) have been clarified by years of probing discussions and actual field experience.

THOROUGHNESS: The robot will cover the programmed inspection path or area completely, with a uniformly high level of concentration.

CORRECTNESS: The robot will deploy the correctly set up inspection instrument using exactly the programmed deployment protocol.

RECORDABILITY: The robot will faultlessly remember the location and result of every measurement*.

* It will presumably not elude the astute reader that the legal departments of commercial airlines may regard recordability and recording as not entirely desirable features; in the military aviation sector, however, they are usually favorably regarded.

With robotic deployment the correct data will always be available for interpretation (by computer software or by human experts), the location on the airplane where the data were obtained will always be known exactly (enabling advanced “C-scan” image-accumulation-and-display whatever the sensor), and precise trend analysis over arbitrary time periods will become possible (enabling better understanding of the development and evolution of problems, and allowing the operator and the regulatory authorities to choose statistically appropriate inspection intervals).

4. ANDI AND CIMP

4.1. ANDI: AUTOMATED NONDESTRUCTIVE INSPECTOR

The FAA Aging Aircraft Research program sponsored the design, construction, and testing of the Automated NonDestructive Inspector (ANDI) at CMU in a joint project of the Carnegie Mellon Research Institute (CMRI), the university’s applied research arm, and our lab, the Intelligent Sensors, Measurement, and Control Lab, in the Robotics Institute of the School of Computer Science. ANDI’s design was dictated by the FAA’s state of mind and by the state of NDI technology around 1990, when the project was defined and begun. The state of mind at the time, still dominated by Aloha’88, was that large scale eddy current “fishing expeditions” are a desirable way to head off future “Alohas”, and that large scale instrumented inspection could be made palatable to commercial airline operators if there were an economically acceptable automated device to deploy the sensors. We considered three broad design families for the robot’s mobility module. We call these the *car wash*, the *cherry picker*, and the *skin crawler*. These families are described in the sidebar ***design scenarios for robots for aircraft inspection***, in which we also discuss the circumstances of commercial airlines operations and economics that led is to pursue the skin *crawler option* for ANDI.

The state of technology for eddy current sensors at the time was mainly manually manipulated pencil probes and complex impedance plane oscilloscope displays of their signals. These circumstances led to a design for ANDI that maneuvers most gracefully along fore-aft lines of rivets, maintaining precision alignment with them so that an eddy current pencil probe scanned parallel to the line of motion would follow the desired scanning path with little or no need for finely tuned closed loop path control.

The design developed for this scenario[4,6] is drawn on the left side of Figure 2; to the right of the drawing is a photograph of the near-final ANDI on a DC-9 nose section at the Aging Aircraft Nondestructive Testing Center (AANC, Sandia National Laboratories, Albuquerque NM). This design, a form that is known in the robotics literature as a “beam walker,” achieves mobility by suitable motions of the bridges (arms) relative to the spine as the suction cup groups on the spine and the bridges are alternately affixed and released. The eddy current probe is scanned by one of the bridges moving along the spine while the spine’s suction cups are affixed to the aircraft skin. ANDI is equipped with four cameras for navigation and alignment: one each fore and aft to align the spine with the rivet line, one adjacent to the eddy current probe to verify location and alignment, and one high mounted with a wide angle field of view for navigation, obstacle avoidance, and proprioception (“self awareness”). In contrast to CIMP, the second CMU aircraft inspection robot (Section 4.2), whose capability is focused on enhanced remote visual inspection, ANDI's cameras were not intended to have sufficient resolution to be useful for visual inspection per se.

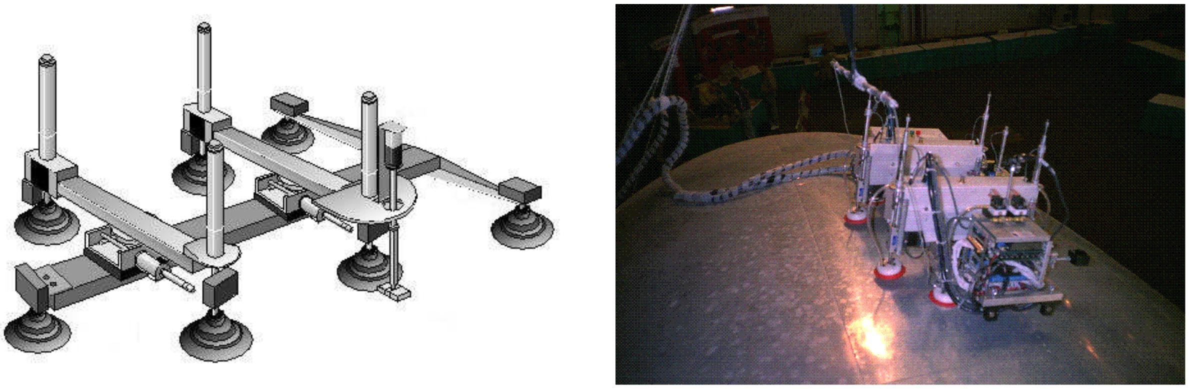

Figure 2: (left) ANDI as a design drawing, and (right) photographed on the nose section of a DC-9. In the drawing, the eddy current sensor is seen on the near end of the far bridge (arm). In the photo the small black box (on an outrigger on the far side) contains one of the two alignment cameras (see text for discussion of camera arrangement).

Despite essential successes in mobility (getting where it needed to be), automatic alignment (using a machine vision rivet line finding algorithm), manipulation (moving the eddy current probe smoothly along the desired path), and measurement (collecting and delivering eddy current sensor data to the ground), as well as the articulation of a comprehensive system architecture for integrating robotics and automation into aircraft maintenance and inspection, unforeseeable changes in the context for ANDI led to its early marginalization.

First among these factors was a de facto return to the pre-Aloha'88 model, which says that visual inspection should be the lion's share of skin inspection, with eddy current and other NDI technologies being used for backup, confirmation, and a relatively small number of directed inspections for specific flaws at specific problematic locations. A robot designed for large area eddy current inspection along rivet lines would have a hard time being economically competitive in an environment that views eddy current as a confirming technology for suspected visual flaws and as a survey technology only for a few specific fuselage locations, e.g., locations known from structural models or past experience to present specific cracking or corrosion patterns.

Simply stated, at least in the civilian sector, there is no economic interest in a robot that does the 10% of inspections that are instrumented; to make an impact with the commercial airline operators, a robotic inspection system will have to do the visual inspections that account for 90% of the inspection effort.

Another development that weighs substantially against the viability of ANDI is the recent advance in sensors and display systems for C-scan rendering of eddy current data. We now have linear and area arrays (or their equivalent in, e.g., magneto-optic imaging (MOI), mentioned in sidebar ***instrumented (NDI) inspection: how it works***), and inspectors now expect to see false-color images rather than oscilloscope traces, making ANDI's mechanical optimization for point probes somewhat pointless.

4.2. CIMP: CROWN INSPECTION MOBILE PLATFORM

CIMP, built in our laboratory with support from the Ben Franklin Technology Center of Western Pennsylvania and our spin-off company Aircraft Diagnostics Corporation, is an aircraft inspection robot that is explicitly *not* a "wall crawler." Chastised by the two lessons of ANDI:

if you spend all your time working on the robot's mobility you'll never get any

Mel Siegel <mws@cmu.edu> / The Robotics Institute / Carnegie Mellon University /Pittsburgh PA 15213 USA / 412 268 8802 / FAX 412 268 5569

inspection data

and

if you can't do visual inspection nobody will be interested in your robot,

we set out to demonstrate that a robot could generate data, first and foremost video data whose quality inspectors would gladly accept for routine visual inspection, and to deliver the data to an "inspector's workstation" off the airplane. To allow us to concentrate on inspection data and not inspection equipment transportation, we designed[7] an interim robot whose mobility is limited to the fuselage crown: CIMP, the Crown Inspection Mobile Platform, shown in Figure 3.

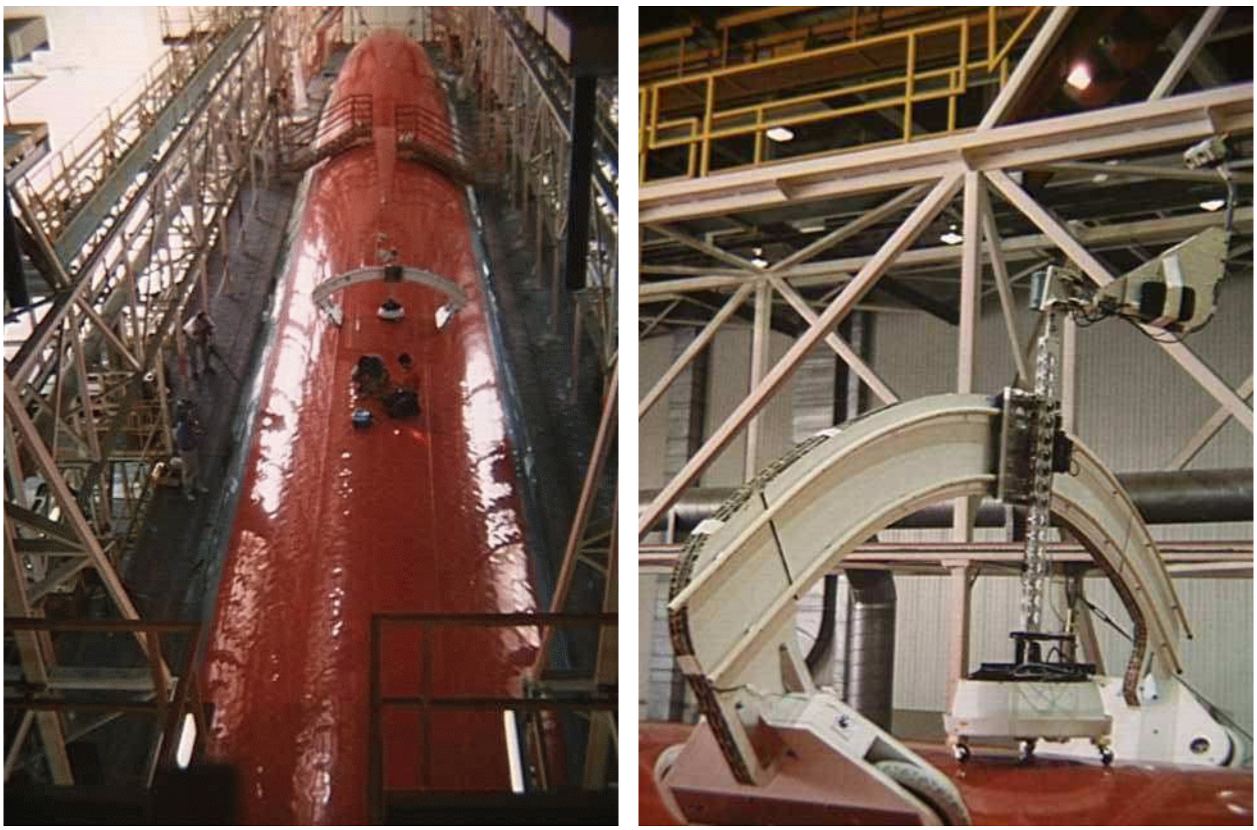

Figure 3: (left) CIMP on a 747 in a heavy maintenance bay at Northwest Airlines' Minneapolis headquarters. The inspector, observed by a CMU staffer, is performing an eddy current check of a visual anomaly detected using the remote vision system shown in sidebar ***remote 3d-stereoscopic visual inspection***. Future CIMP models would incorporate remotely operated eddy current sensing. (right) CIMP showing mobility (differentially driven wheels), sensor pod mounted off circumference-scanning carriage, and wide angle cameras for proprioception and navigation (upper right). The vertical stalk and the sensor pod rotate to change the camera viewing azimuth.

Because CIMP works with gravity instead of against it, it does not need a tether. It was designed for the curvature of a DC-9, and for window-line to window-line mobility on that aircraft type; however it turned out to be more convenient to test the prototype on a 747, on which it ran with no difficulty despite having the "wrong" curvature.

Because its power requirements are tiny compared to a robot that has to adhere to the fuselage in arbitrary orientations, CIMP does not need an umbilicus. It runs for several hours on its internal batteries; exactly how long depends on the variable demands of mobility, manipulation, illumination, etc. Control signals are transmitted to CIMP wirelessly using off-the-shelf model airplane transmitter technology. Video data are returned wirelessly using micropower radiofrequency channels; in the prototype these are off-the-shelf 2.4 GHz cable eliminators sold in the consumer market to wirelessly connect a home VCR and TV. In a commercial version of CIMP somewhat more sophisticated (and costly) channel options would be appropriate to avoid signal degradation due to multipath effects.

CIMP has been successfully operated on a 747 at Northwest (as shown in the accompanying figures) and on a DC-9 at US Airways. Working aircraft inspectors have been uniformly enthusiastic about the quality and utility of the imagery that the CIMP remote 3D-stereoscopic video system delivers. However many are skeptical about the economic benefits that might reasonably be expected from robotic deployment of inspection equipment. Some also question whether the introduction of robotic deployment equipment would enhance their job satisfaction; despite our best intentions to make the inspector's job easier, safer, etc., by "getting the man off the airplane", several inspectors have told us that they like their jobs in large part because they like being on the airplane.

4.2. 1 CIMP's "INSPECTOR's CONSOLE"

CIMP's user interface, the "inspection console", provides for remote 3D-stereoscopic visual inspection of the aircraft surface, and for remote control and navigation of CIMP on the aircraft crown. The current prototype inspection console consists of two primary displays and their supporting equipment and a radio transmitter (of the type used to control model vehicles) that controls forward and backward motion, left right steering, camera position and orientation, and lighting selection and orientation. The first display is a monitor that delivers live video at NTSC spatial and temporal resolution to eye, providing stereoscopic imagery of either the inspection or the navigational camera pair. The second display is a Silicon Graphics Indy workstation with a GUI (graphical user interface) that we call the Intelligent Inspection Window (IIW). The IIW fulfills a variety of requirements: it displays the live monoscopic or still stereoscopic imagery; it is the operational interface and output display unit to the image enhancement and understanding algorithms (activated by the menus and buttons of the IIW); and, in the future, it will contain facilities for creating, editing, storing and retrieving multimedia records of surface defects. 3D-stereoscopic image pairs showing different aircraft skin features, the sensor pod containing the 3D-stereoscopic cameras, and an inspector at the console are shown, along with additional technical details, in the sidebar ***remote 3d-stereoscopic visual inspection***.

5. SKIN DEFECT DETECTION AND CLASSIFICATION

5.1. BACKGROUND

To our surprise and delight, aircraft inspectors have been spontaneous and enthusiastic advocates for using computer image enhancement and automated image understanding for flaw detection; they are, however, skeptical about the likelihood that we will succeed at the latter.

The goal of an image understanding algorithm for aircraft inspection is to recognize and classify certain surface flaws that might appear in the live imagery. The recognition capability of an algorithm is achieved by correlating features of the imagery with prior or learned knowledge of the surface flaw types. However, developing a successful image understanding algorithm remains a non-trivial challenge, due primarily to the difficulty of generalizing and encoding in an algorithm the notions that humans use to discriminate normal from defective, the limited resolution and dynamic range of practical imaging systems, and the confounding effects of environment factors such as illumination.

Given these limitations, an attractive scenario for application of image understanding algorithms in remote visual inspection is screening large volumes of image data. The image understanding algorithm can conservatively label all plausible defects, as a coarse prefilter for the inspector who does the fine screening. Another scenario is the interactive use of these algorithms by an inspector to obtain a second opinion about a particular suspicious flaw. This possibility is most attractive when the real-time inspector is relatively inexperienced, in general or with respect to a specific problem, compared to the inspectors whose expertise has been incorporated (explicitly or implicitly) in the algorithm; in this scenario the computer fulfills a training role in addition to its direct inspection role.

In the spirit of these anticipated operating scenarios, we have developed prototype algorithms[7] that detect surface cracks, surface corrosion, and subsurface corrosion evidenced by surface pillowing.

5.2. CRACK DETECTION ALGORITHM

The crack detection algorithm that we have developed is modeled closely on the inspectors' practice of using grazing angle directional lighting to enhance crack visibility. We emulate the directional lighting produced by an inspector's flashlight by employing a remotely controlled rotatable directional light source on CIMP. The remote inspector can rotate the light source around a rivet location and examine the resulting live monoscopic or stereoscopic imagery of the rivet and its neighborhood for cracks. In addition, the inspector can run the crack detection algorithm on these images for detection or verification of cracks in the live imagery. The stereoscopic imagery can also be recorded (at slightly reduced resolution) on a standard S-VHS recorder for future examination or computer processing.

The first module of our crack detection pipeline finds rivets in the image presented to it. Since cracks appear in the neighborhood of rivets, finding rivets in the first stage permits subsequent states to focus on the areas ("regions of interest", ROIs) that are most likely to contain cracks. Rivets are identified by detecting the circular arc edges made by their heads; a region of interest is then defined as a square centered on a rivet. Figure 4 shows a section of an aircraft surface with three simulated cracks appearing as dark lines emanating horizontally from the two rivets, and the two ROIs found by the algorithm.

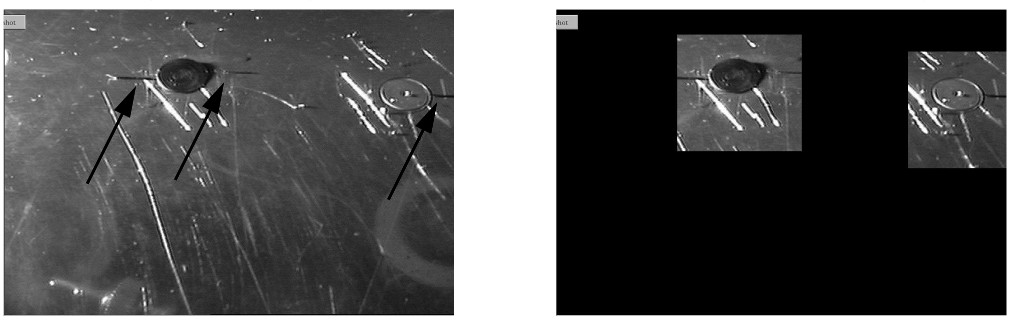

Figure 4: Rivet "region of interest" (ROI) finding algorithm. (left) Aircraft skin showing two rivets. Arrows point to three short black horizontal lines (hairs from a fine brush) that simulate narrow cracks. (right) ROIs found by the algorithm. Notice reasonable behavior even for a rivet near the edge of the frame.

Even the relatively small areas defined as ROIs still typically contain many edge-like features, most of which are due to rivet edges, scratches, dirt marks, lap joints, metal repair plates, and a few of which are due to real cracks. Thus for the second stage in the crack detection pipeline we need an algorithm that finds and attaches a quantitative description to each edge, and for the third stage an algorithm that discriminates the small fraction of edges that are cracks from the many edges that are of no interest.

A crack is typically very small compared to most visible features of the aircraft surface; this motivates us to develop, for the second stage, a multiscale (also called multiresolution) algorithm to detect edges based on quantitative spatial features of edges. For this stage we use wavelet filters (discussed in more detail in Section 5.3 in the context of surface corrosion detection) to project an ROI to different resolutions, and estimations of intensity variation at each resolution for multiscale edge detection. Edges of the same object or feature are usually present in more than one scale. We use a coarse-to-fine edge linking algorithm to attach a *propagation depth* to each edge appearing at the coarsest scale. The propagation depth, and several additional features of the edge, are taken to comprise a feature vector that can be used to classify the edge to be a crack or to be “crack-like but non-crack”.

The classification is done in the third stage by a simple neural network trained on a set of feature vectors that had been identified by a person as corresponding to either a crack or a non-crack. The result of applying this pipeline to the area around a badly damaged rivet hole is illustrated in Figure 5.

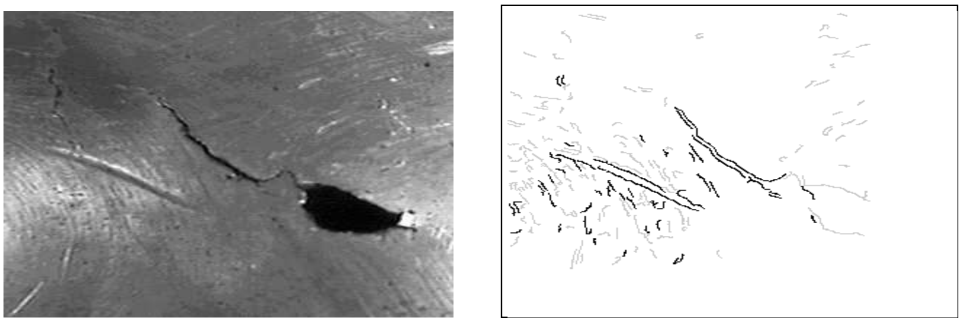

Figure 5: (left) Photograph of a badly damaged rivet hole with a large crack and a deep, crack-like dent. (right) Output of the crack detection algorithm, with crack-like edge features shown in dark gray and non-crack-line edge features shown in light gray. [This is a very severe example; really interesting cracks are so small, in length or openning or both, that they would be invisible when printed at this resoution.]

5.3. SURFACE CORROSION DETECTION ALGORITHM

A comprehensive corrosion detection algorithm needs to detect both surface and subsurface corrosion. Surface corrosion is detected by color and texture visually suggestive of corrosion, whereas subsurface corrosion is detected by distortion (“pillowing”) of the surface. Thus a comprehensive algorithm requires an image and a shape profile of the inspection surface to detect both types of corrosion. In this section, we describe the algorithm we have developed to detect surface corrosion; in the next section we describe our subsurface corrosion detection apparatus and algorithm.

We detect surface corrosion by a binary segmentation of the image into regions of texture suggestive of corrosion and regions of texture suggestive of freedom from corrosion. We implement the segmentation via a surface description that uses multiresolution-multiorientation wavelet functions to compactly represent the scale and orientation of texture in small surface patches. Since wavelets have good spatial and frequency localization, the wavelet coefficients provide the compact representation of texture that we seek.

In our most recent and refined implementation of this approach, the raw 24-bit RGB images are, in the first module, transformed into corresponding YIQ representation. Then we perform a three-level discrete wavelet transform (DWT) without sub-sampling of the Y-channel (luminance), and a two-level DWT with sub-sampling separately of the I- and Q-channels (chrominance components). The sub-sampling of the DWT of the Y-channel forces the Y-channel decomposition to be translationally invariant, which is a desirable feature for texture recognition. The DWTs decomposes the Y-channel into ten sub-bands and the I- and Q-channels each into seven sub-bands. Each sub-band corresponds to a particular texture scale

Mel Siegel <mws@cmu.edu> / The Robotics Institute / Carnegie Mellon University /Pittsburgh PA 15213 USA / 412 268 8802 / FAX 412 268 5569

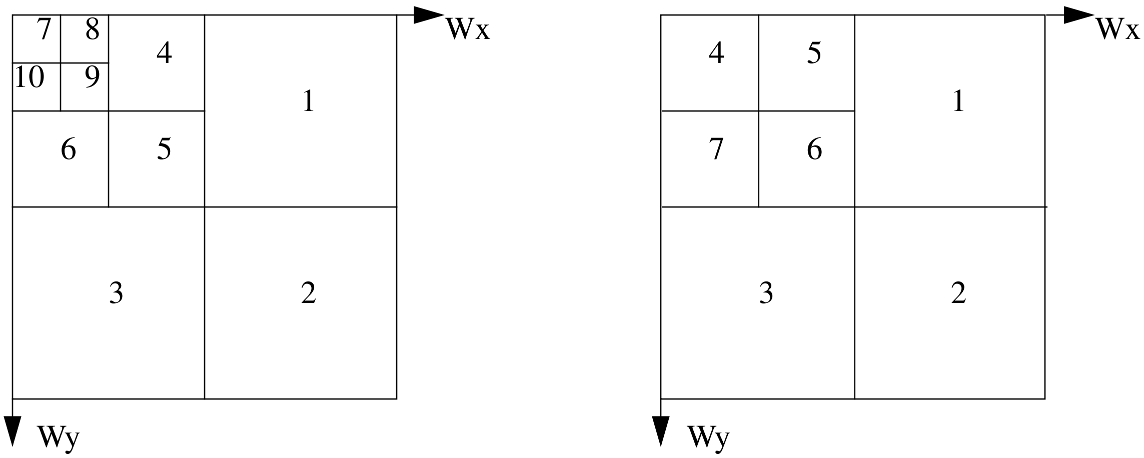

Figure 6: Sub-band decomposition of images based on texture scale and orientation. Smaller squares correspond to smaller spatial frequencies; the square adjacent to the origin is the DC component. Different squares of the same size correspond to different orientations at the same scale. (left) Y-channel contains the luminance information; 3-level DWT gives 10 sub-bands. (right) I- and Q-channels contain the chrominance information; 2-level DWT gives 7 sub-bands

and orientation, as shown shown in Figure 6. The actual wavelets we use are derived from the Battle-Lemaire 32-tap asymmetric FIR filter[9].

In the second module, feature extraction, we calculate for each 32-by-32 non-overlapping block in the YIQ image, a vector of ten features. These are a subset of seven features extracted from the Y-channel decomposition and three extracted from the I- and Q-channel decompositions. Included in the Y-channel feature set are three rotationally invariant energy measures and three rotationally invariant orientation measures, plus the DC sub-band energy, sub-band seven in Figure 6. [“Energy” is defined as the weighted sum squared of the wavelet coefficients belonging to that block.] The three features from the I- and Q-channels are the I-to-Q ratios of the total energy in sub-bands 1, 2, and 3, in sub-band groups 5, 6, and 7, and in DC channel 4. Summing over sub-bands of the same scale averages over orientations, i.e., it removes sensitivity to viewing azimuth.

In the last module, we use a three-layer feed-forward neural network (10 inputs, 30 hidden layer neurons, 2 outputs) to classify the preceeding feature vector as either corresponding to a region of corrosion and or corresponding to a region non-corrosion. The neural network was trained using a training set hand-classified vectors.

Figure 7 displays, on the left, an image that includes both corroded and uncorroded aircraft skin removed from an airplane as part of a maintenance program, and on the right, the output of our surface corrosion